View metadata, citation and similar papers at core.ac.uk
brought to you by CORE
provided by Carolina Digital Repository

ABSTRACT

Dissolved Rare Earth Element (REE) fractionation mechanisms in freshwater samples have been parameterized by lab experiments and measured in major world rivers. To confirm whether results from controlled lab experiments are reciprocated in small-scale natural systems, I analyzed REE contents in water samples from groundwater springs and streams on San Cristóbal Island, Galápagos. The island is comprised of essentially a single lithological unit (Ocean Island Basalt) and exhibits a steep hydrological gradient on the windward slope over a short spatial extent which results in a wide range of physicochemical and dissolved mineralogical properties of water. This allows for the investigation of factors exerting primary control on REE fractionation without the influence of changing lithology. Samples show a wide range of pH (5.5-8.2) associated with changes from Mn-dominated dissolved fractions to Fe-dominated as pH increases. Local basalt-normalized REE patterns exhibit a wide range ($[La/Yb]_b$ = 0.41-1.78 and $[Ce/Ce^*]_b$ = 0.58-2.12) for the small areal extent of the watershed (~ 13 sq. km). Comparisons between "dissolved" load (<0.45µm) and "soluble" load (<0.02µm) data demonstrate the importance of colloidal-sized metal species in aqueous solution. The difference of REE results between the "dissolved" load data are attributed to contrasting fractionation from opposing aqueous mineralogical systems (Mn vs. Fe) present across the watershed, consistent with laboratory studies.

1 INTRODUCTION

Rare Earth Elements (REEs) in natural waters can serve as geochemical tracers of erosional processes (Goldstein and Jacbosen, 1987; Allègre et al., 1996; Gaillardet et al., 1997) and paleoenvironmental conditions (Kato et al., 2002; Liu et al., 1988; Murray et al., 1990). These direct applications of REEs in marine water and sediment samples require proper parameterization of inputs into the ocean by chemical weathering and transport from continental sources. REE fluxes to the ocean remain poorly understood at the global scale (Bertram and Elderfield, 1993; Tachikawa et al., 2003; Arsouze et al., 2009). To estimate the oceanic REE budget, continental weathering fluxes must be investigated in order to constrain REE behavior before and during transport to the ocean.

Dissolved REE concentrations in continental waters are primarily sourced from the underlying bedrock (Steinmann and Stille, 2008; Smith and Liu, 2018) but can fractionate relative to each other due to several factors. All are trivalent except for Ce and Eu, which can be tetravalent and divalent, respectively. REEs also exhibit a "lanthanide contraction:" as atomic number increases, the atomic radii progressively decrease as the 4f electron orbital is filled. Distinct fractionation patterns can occur during geologic processes as a result of these relative differences between behavior of REEs. The most commonly cited mechanisms for REE fractionation include differential release during chemical weathering, variable stabilities of aqueous complexes, and adsorption to sediment particles or binding with colloids (Xu et al., 2009; Cantrell and Byrne, 1987; Johannesson et al., 1995; Sholkovitz et al., 1995; Dia et al., 2000).

Numerous laboratory experiments have allowed for the exploration of REE fractionation mechanisms in aqueous solution, most of which indicate that a significant amount of fractionation is induced on the surface of MnO_2 and Fe-oxyhydroxide particles (DeCarlo and Wen 1997; Bau et al., 1999; Ohta and Kowabe, 2001). The efficiency of particulate scavenging of REEs has been shown to depend on pH, particulate mineralogy, ionic strength of the solution, and redox potential. Because ionic strength and redox potential do not have broad ranges of variability in surficial freshwater systems, the dominant factors we focus on are pH and particulate mineralogy. While there is a large amount of literature on REE speciation in large freshwater river systems and estuaries (Goldstein and Jacobsen, 1988; Dupré et al., 1996; Gaillardet et al., 1997), few studies have been performed on smaller catchments of a single bedrock lithology which exhibit a wide range of variability in climate and soil mineralogy.

The Galápagos Islands can be thought of as a natural laboratory (Percy et al., 2016) in which certain environmental variables are controlled (consistent bedrock chemistry, no geothermal activity) while hydrochemical variables (rainfall, pH, chemical weathering) show dramatic changes across a small area. This study is intended to 1). investigate whether REE fractionation mechanisms observed in a laboratory (where all variables are strictly controlled) are represented in a small natural system such as this, and 2). compare the observed trends in this small catchment to much larger river basins.

2 METHODS

2.1 Setting

The island of San Cristóbal (Figure 1a) is part of the Galápagos Archipelago, a set of volcanic islands ~1000 km off the coast of Ecuador which formed from hotspot volcanism (Hey and Vogt, 1977). San Cristóbal, the oldest major island of the archipelago, first emerged 2.35 ± 0.03 m.y.a and has not had significant volcanic activity in about 10,000 years. Basaltic flows are predominantly alkaline, with thick pyroclastic flows at the summit (Geist et al., 1986; White et al., 1993).

A steep topographic gradient induces orographic precipitation at high altitudes, creating a distinct precipitation gradient from wet to dry with decreasing elevation. At high elevations, precipitation occurs year round either as rain in the wet season (January to June) or fog in the dry season (June to December), whereas lower elevations infrequently received precipitation during the wet season only. The effects of this climate gradient are clearly observed because of the small areal extent of the island: soils in high altitude areas of the windward slope exhibit low hydraulic conductivity (10^{-5} - 10^{-6} m/s) and porosity (15-25%) while lower altitude areas show much higher values for both properties (10^{-3} - 10^{-4} m/s and 35-40%, respectively) (Adelinet et al., 2008). Changes in physical soil properties are accompanied by shifts in dominant clay mineralogy as well, with gibbsite and other products of intense chemical weathering appearing in high altitude soil samples but absent in the lower altitude samples (Adelinet et al., 2008; Ingala et al., 1989).

Numerous freshwater springs can be found on the island, some of which are used by local residents as a water source. Recent studies use field measurements, aerial geophysical surveys, and geochemical studies to characterize the hydrogeologic system on San Cristóbal - all results indicate a system including dike impounded aquifers, a basal aquifer, and several perched aquifers which form contact springs at their intersection with topography (Violette et al., 2014; Pryet et al., 2012; Warrier et al., 2012). The majority of the island is occupied by Galápagos national park with limited agricultural use in the wet highlands areas around the summit. Farmers generally use sustainable agricultural practices,

and the lack of industrial facilities drastically lowers the possibility for anthropogenic contamination of freshwater sources.

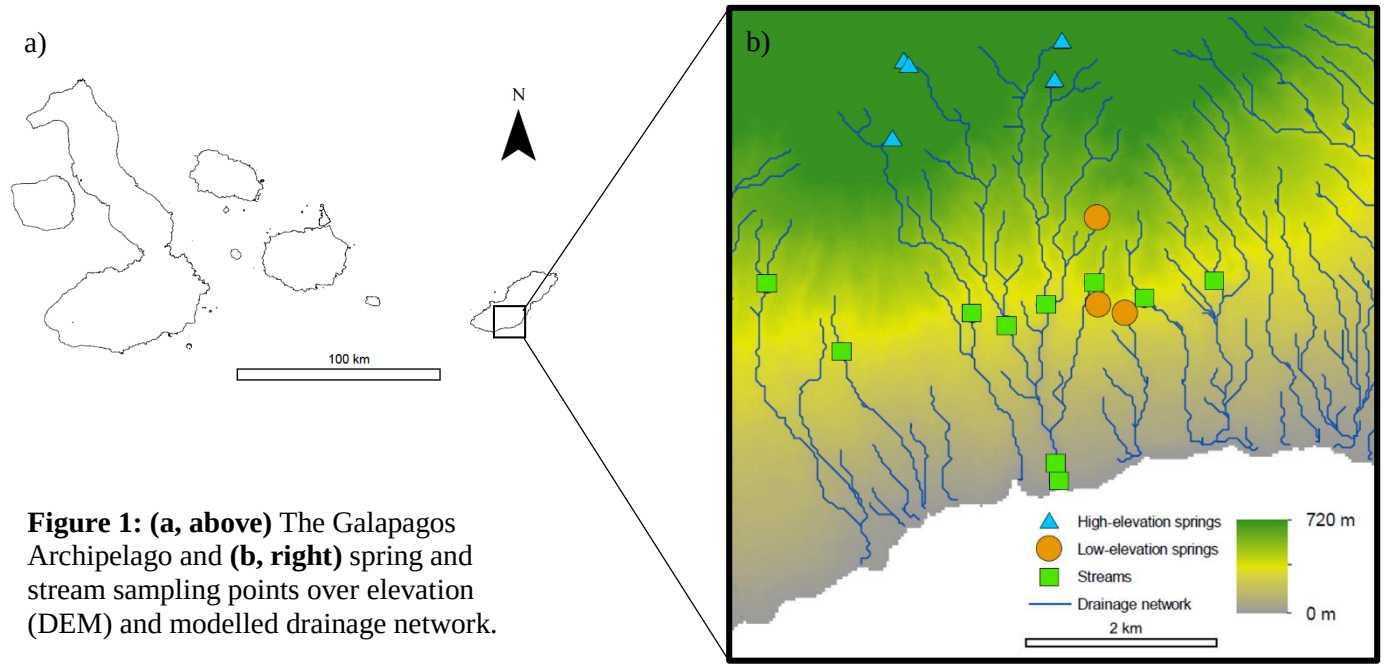

Figure 1: (a, above) The Galapagos Archipelago and **(b, right)** spring and stream sampling points over elevation (DEM) and modelled drainage network.

2.2 Sampling

17 water samples were taken during May and June 2017 across several catchments over a total area of approximately 13 sq km (Figure 1b). Of these, 8 were groundwater springs and 9 were surficial streams. In addition to these freshwater samples, one sample was taken from a small estuarine mixing area at a stream outlet and two seawater samples were taken.

Measurements of pH, temperature, and total dissolved solids (TDS) were taken on-site using a Oakton “PT Testr” meter. Samples were filtered immediately using 0.45µm filters (Sterlitech™ polyethersulfone membrane) and collected into pre-cleaned beakers. 4 samples were selected to undergo additional filtration through 0.02µm filters to investigate partitioning within the "dissolved" load (< 0.45µm) into the colloidal phase (between 0.02µm and 0.45µm) and soluble phase (< 0.02µm). After filtration and transport, all were acidified to pH < 2 using double-distilled nitric acid and stored at 4ºC to await analysis for REEs.

2.3 Chemical Analysis

Water samples were analyzed for major cations and REEs using an Agilent™ 7900 Quadrupole Inductively Coupled Plasma Mass Spectrometer (Q-ICP-MS) at the Plasma Mass Spectrometry (PMS) Laboratory at University of North Carolina - Chapel Hill. Prior to analysis samples were concentrated 10-20 times by evaporation and re-dissolved with 2% v/v double-distilled nitric acid, accompanied by a blank through each process. An internal standard contains 10ppb ^{115}In are used to correct instrumental drift. Calibration standards of 1 ppt, 10 ppt, 100 ppt, 1 pbb, and 10 ppb REE concentrations were prepared from single element standards purchased from Inorganic Ventures™. I have analyzed the certified reference material for river water (SLRS-5) from the National Research Council of Canada to evaluate accuracy of analysis. Isobaric interferences from oxides were monitored during ICP-MS analysis, with oxide presence in the plasma stream controlled to be less than 1% in no-gas mode and 0.3% in He collision cell mode.

Repeated analyses (n=4) of the river water standard SLRS-5 yielded values with accuracy ranging from 0.8% (Ho) to 21.2% (Lu), averaging to 5.4% accuracy compared to the certified and literature values (Yeghicheyan, 2013). On average, REE values for each sample had RSD (Relative Standard Deviation) between 2.6% (La) and 15% (Lu) with most REEs below 5% RSD.

3 RESULTS

3.1 Major chemical composition

Measured field parameters (pH, TDS, and temperature) are listed in Table 1, along with major chemical data and the modelled Saturation Index (SI) of amorphous Fe-oxyhydroxide. Measured pH values ranged from moderately acidic (pH=5.5) in high-elevation springs to mildly basic (pH=7.9) in low-elevation springs and streams. Measured TDS values exhibited similar patterns, with low TDS values in high-elevation springs (TDS=10 mg L^{-1}) and increased to more concentrated values (TDS=79 mg L^{-1}) at lower elevation. The wet-dry gradient associated with elevation described previously is evidenced by these sharp changes in pH and TDS, both of which increase with water-rock interaction downslope.

Significant change in stream chemistry is observed in terms of major cations concentrations, increasing from ~0.1 mg/L to ~10 mg/L downslope.

All high-elevation springs had relatively high Mn concentrations (4-30 ppb) due to their low pH (5.5-6.5). All streams and low springs exhibited positive SI for Fe-oxyhydroxide while the majority of high springs showed negative values. This suggests that Fe-oxyhydroxide precipitation is not thermodynamically favorable in high-elevation springs. There is a positive correlation between SI Fe-oxyhydroxide and pH with one notable exception. The high-elevation spring sample CG-1 shows a much higher SI Fe-oxyhydroxide than expected despite its relatively low pH due to its high concentration of Fe. It is important to emphasize the distinct mineralogical gradient observed across the elevational gradient from dissolved Mn-dominant waters at high altitudes to descending to dissolved Fe-dominant once pH is sufficiently high.

Dissolved Organic Carbon (DOC) was analyzed using a Shimadzu Total Organic Carbon Analyzer in early 2018, several months after sample collection. The amount of time that passed between sampling and analysis prevents any conclusion from being confidently made from absolute DOC values. However, general trends may still be observed for the range and relative values between samples. The overall variability of the samples was low, with DOC < 2ppm for all samples. Measured DOC does not correlate well with other variables such as the SI of Fe-oxyhydroxide or REE ratios described in section 3.2.

	Elevation	pH	TDS	Temperature	Na	Mg	K	Ca	P	Al	Fe	Mn	DOC	SI FeOOH
	[m]		[mg/L]	[°C]	[mg/L]	[mg/L]	[mg/L]	[mg/L]	[µg/L]	[µg/L]	[µg/L]	[µg/L]	[mg/L]	
High springs														
CG-1	520	6.4	48	19.9	2.08	1.29	0.10	1.59	6.10	2.80	1687.31	138.79	1.1	1.54
CG-2	510	6.5	36	21.2	3.33	2.19	0.34	3.11	7.13	3.06	7.85	4.01		-0.48
Lt-1	524	5.9	17	20.2	2.87	0.51	0.16	0.52	7.31	25.27	31.67	7.50		-1.61
Lt-2	570	5.5	22	19.5	3.13	0.53	0.39	0.83	4.92	16.48	67.01	28.24	0.8	-2.53
Lt-3	572	5.6	10	22.5	2.33	0.35	0.18	0.48	6.92	77.57	37.52	20.74	2.1	-2.38
Low springs														
CG-6	313	7.8	68	21.8	6.69	5.51	0.75	8.22	55.54	15.64	22.69	0.61		2.38
CG-8	283	7.4	70	21.7	6.46	4.58	0.93	6.52	35.14	7.01	5.83	0.09	0.5	1.58
CG-9	237	7.7	79	22.2	10.69	7.50	1.26	8.43	33.80	10.48	29.09	0.95	1.1	2.44
Streams														
CG-3	190	7.9	80	21.5	6.85	7.28	1.65	8.69	42.11	31.41	57.04	0.42		2.81
CG-4	223	7.6	68	21.5	5.25	4.77	0.64	6.54	37.33	9.06	27.09	0.50	0.9	2.41
CG-5	253	7.8	79	21.5	3.96	3.51	0.63	6.16	45.79	85.33	89.20	0.82	1.9	2.99
SE-1	174	7.8	65	20.7	5.82	4.88	0.43	6.38	11.90	2.07	6.44	0.21		1.89
SE-2	195	7.3	30	22	4.26	1.60	0.10	1.86	9.39	2.93	3.94	1.72		1.30
SE-3	183	7.2	48	21	6.14	2.90	0.40	3.33	22.63	4.79	31.00	8.60		2.03
SE-4	18	7.2	56	25.2	8.25	2.84	0.52	3.07	10.36	1.64	7.35	1.20	0.5	1.32
TP-1	202	7.3	37	21	4.51	2.08	0.39	2.61	7.55	9.53	37.56	8.44	1.2	2.31
TP-2	307	8	50	20.2	5.00	3.12	0.43	4.69	21.27	11.30	13.58	0.48		2.28

Table 1: Field parameters and major chemical data

3.2 REEs

Rare earth element concentrations are listed in Table 2 for the "dissolved" (<0.45μm) fraction. Total REEs in the dissolved load are generally low, ranging from 10-300 ng L^{-1} with an average of ~100 ng L^{-1}. The highest total concentrations of REEs were found in low elevation streams, but no correlation can be made between total REEs and elevation because of the wide spread of values across the entire topographic profile. For many samples, Lu is omitted because the uncertainty was too high (>10% RSD).

To compare measured dissolved load REE concentrations with other similar studies, we normalize our samples to a bulk continental crust REE pattern (Figures 2a-c). Normalized to Post Archaean Australian Shale (PAAS), samples show depletion in LREEs in the dissolved load, comparable to other studies of basalts and catchments draining basalts (Taylor and McLennan, 1985; White et al., 1993; Steinmann and Stille, 2008; Johannesson et al., 2017). No significant MREE enrichment can be observed, with mostly flat patterns between Eu and Lu. Considering the entire study area is under essentially the same host lithology. Therefore, it is more appropriate to normalize samples to the local bedrock to investigate relative fractionation patterns associated with chemical weathering. Average REE values from analyzed basalt samples (n=5) are used (White et al., 1993) as the basis of normalization (Figures 2d-f).

To quantify rare earth element fractionation, ratios between abundances of individual elements are compared between normalized samples. The basalt-normalized ratio of La vs. Yb (i.e. $[La/Yb]_b = [La/Yb]_{sample} / [La/Yb]_{basalt}$) allows for the quantification of LREE enrichment or depletion relative to HREE. Collected samples show a wide range of $[La/Yb]_b$ (0.41-1.78) over the study area, showing extreme LREE depletion and enrichment across varied environmental conditions. To explore the unique behavior of Ce due to its 4+ valence state, the ratio defined as the "Ce anomaly" is used to compare observed Ce concentrations to hypothetical Ce concentrations based on its nearest neighbors ($[Ce/Ce^*] = [Ce/(La*Pr)^{0.5}]$). $[Ce/Ce^*]_b$ values for streams and low springs were typical in comparison to similar conditions with negative Ce anomalies between 0.58-1.02, showing removal of Ce from the "dissolved"

phase. High elevation springs, however, show positive Ce anomalies of up to $[Ce/Ce^*]_b = 2.12$, showing enriched Ce concentrations in the "dissolved" phase relative to La and Pr. Positive Ce anomalies have rarely been observed in the <0.45µm phase of freshwater samples, with most observations being in smaller streams (Steinmann and Stille, 2008).

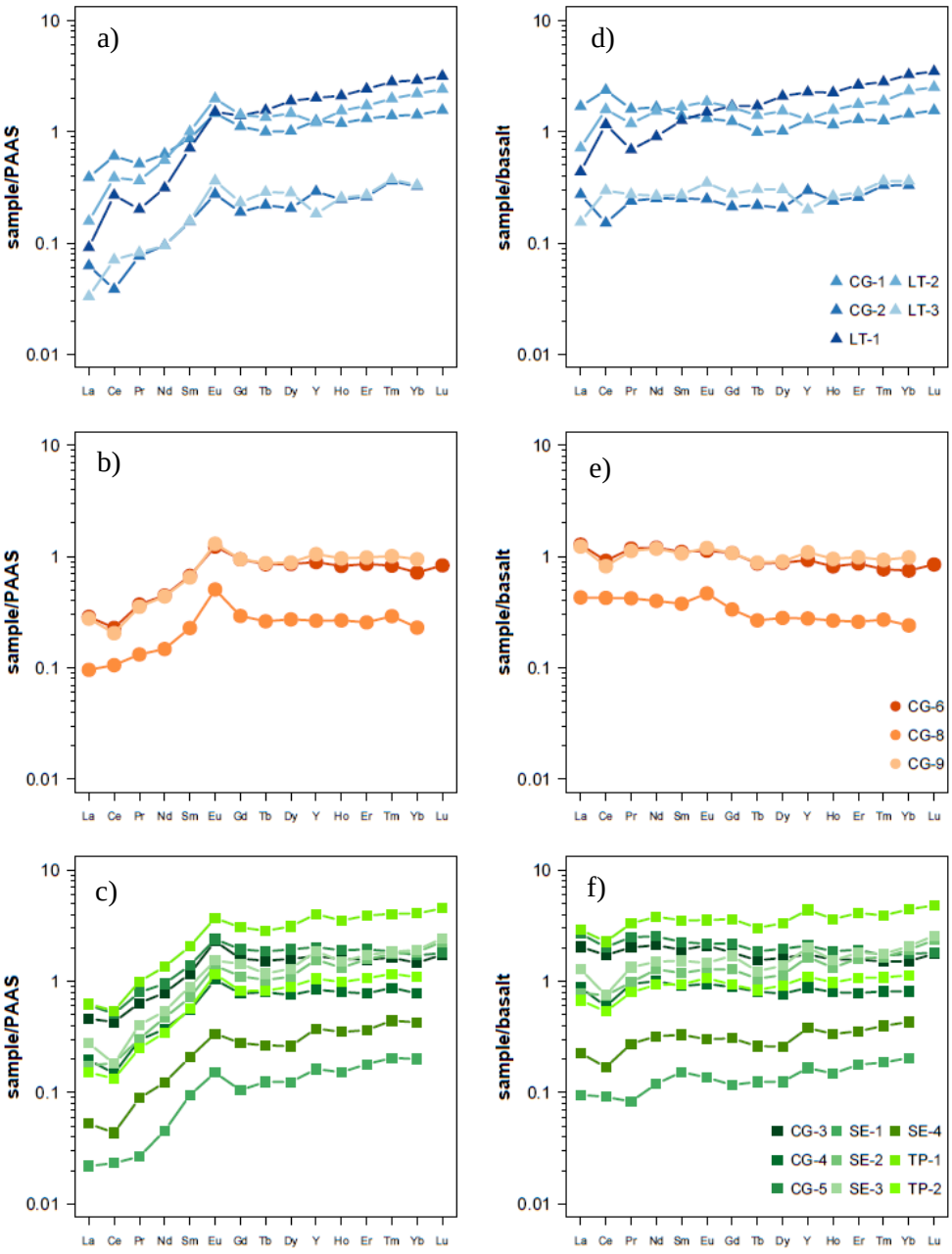

Figure 2: (a-c) Samples normalized to Post-Archaean Australian Shale (Taylor and McLennan, 1985) and (d-f) normalized to average San Cristóbal basalt (White et al., 1993).

	La	Ce	Pr	Nd	Sm	Eu	Gd	Tb	Dy	Y	Ho	Er	Tm	Yb	Lu	$[Ce/Ce^*]_b$	$[La/Yb]_b$	$[Eu/Eu^*]_b$
High springs																		
CG-1	1.69	2.36	1.60	1.66	1.39	1.31	1.24	0.99	1.01	1.28	1.15	1.29	1.26	1.44	1.55	1.44	1.17	1.00
CG-2	0.27	0.15	0.24	0.25	0.25	0.25	0.21	0.22	0.21	0.30	0.24	0.26	0.33	0.33		0.59	0.83	1.08
Lt-1	0.44	1.16	0.69	0.91	1.26	1.49	1.71	1.70	2.09	2.26	2.25	2.63	2.80	3.25	3.48	2.12	0.13	1.02
Lt-2	0.72	1.58	1.19	1.53	1.68	1.86	1.66	1.40	1.53	1.28	1.56	1.77	1.88	2.34	2.51	1.72	0.31	1.11
Lt-3	0.15	0.30	0.27	0.27	0.27	0.35	0.28	0.30	0.30	0.20	0.26	0.28	0.36	0.36		1.44	0.43	1.27
Low springs																		
CG-6	1.28	0.92	1.18	1.20	1.10	1.13	1.08	0.86	0.88	0.93	0.81	0.86	0.77	0.75	0.85	0.75	1.71	1.03
CG-8	0.43	0.42	0.42	0.40	0.38	0.47	0.33	0.27	0.28	0.28	0.27	0.26	0.27	0.24		1.00	1.78	1.31
CG-9	1.23	0.82	1.12	1.18	1.06	1.19	1.07	0.88	0.90	1.09	0.95	0.99	0.93	0.98		0.70	1.25	1.12
Streams																		
CG-3	2.04	1.72	2.02	2.11	1.92	2.10	1.81	1.54	1.62	1.74	1.57	1.58	1.50	1.52	1.76	0.85	1.34	1.12
CG-4	0.88	0.60	0.95	1.00	0.91	0.95	0.89	0.81	0.77	0.88	0.80	0.78	0.81	0.81		0.65	1.08	1.06
CG-5	2.68	2.02	2.50	2.53	2.26	2.17	2.19	1.86	1.96	2.09	1.86	1.93	1.70	1.76	1.81	0.78	1.52	0.98
SE-1	0.10	0.09	0.08	0.12	0.15	0.14	0.12	0.12	0.13	0.17	0.15	0.18	0.19	0.20		1.02	0.47	1.02
SE-2	0.79	0.75	0.98	1.28	1.19	1.28	1.28	1.06	1.14	1.65	1.32	1.61	1.64	1.92	2.34	0.85	0.41	1.04
SE-3	1.28	0.75	1.34	1.50	1.53	1.46	1.70	1.23	1.38	2.02	1.54	1.80	1.76	2.06	2.57	0.58	0.62	0.91
SE-4	0.23	0.17	0.27	0.32	0.33	0.30	0.31	0.26	0.26	0.38	0.34	0.36	0.40	0.43		0.68	0.53	0.95
TP-1	2.90	2.27	3.31	3.80	3.53	3.55	3.63	3.01	3.33	4.38	3.63	4.10	3.91	4.43	4.81	0.73	0.66	0.99
TP-2	0.68	0.54	0.80	0.93	0.94	1.07	0.93	0.83	0.92	1.10	0.98	1.07	1.08	1.13		0.73	0.60	1.14

Table 2: Basalt-normalized REEs (ng/L) and relevant REE ratios

3.3 Sequential filtration

Selected trace element and REE concentrations for the samples additionally filtered through 0.02μm filters are displayed in Table 3a and 3b, respectively. Percent retention in the soluble phase after sequential filtration is shown as the percent change in (<0.02μm) fraction over the (<0.45μm) fraction. Though most other elements analyzed in this study show >90% retention into the soluble phase, Fe and Mn exhibit notable ranges of partitioning, ~10-90% and ~8-63% respectively, between the colloidal and dissolved phase for different samples. For the two high-elevation springs, Mn largely exists in the soluble fraction (>70%) rather than the colloidal phase. Conversely, Fe shows more soluble phase retention (>60%) in the low-elevation spring.

Almost all HREEs exhibited retention in the soluble phase higher than 90%, showing near complete partitioning of HREEs into the soluble phase. On the other hand, lighter REEs showed lower (40-60%) retention into the soluble phase, suggesting partial occupation of the colloidal phase. Specifically, Ce in the stream samples had much lower percent retention (40%) into the soluble phase than its nearest neighbors La and Pr, which demonstrates its tendency towards oxidative scavenging into the colloidal phase due to its 4+ valence state.

	P	Al	Fe	Mn
	[μg/L]	[μg/L]	[μg/L]	[μg/L]
High springs				
LT-1	7.3	25.3	7.50	31.7
LT-2	4.9	16.5	28.2	67.0
Low springs				
CG-6	55.5	15.6	0.61	22.7
Streams				
CG-4	37.3	9.1	0.50	27.1
Retention in soluble phase				
High springs				
LT-1	>90%	>90%	22%	72%
LT-2	>90%	74%	8%	>90%
Low springs				
CG-6	>90%	>90%	63%	20%
Streams				
CG-4	>90%	>90%	39%	12%

Table 3: Concentrations of selected major and trace elements **(a, above right)** and REEs **(b, next page)** after 0.02μm filtration, with % retention (0.02μm)/(0.45μm). Blank spaces under Lu were removed due to high RSD, no filtered samples had <10% retention in the soluble phase.

	La	Ce	Pr	Nd	Sm	Eu	Gd	Tb	Dy	Y	Ho	Er	Tm	Yb	Lu	$[Ce/Ce^*]_b$	$[La/Yb]_b$	$[Eu/Eu^*]_b$
	[ng/L]	[ng/L]	[ng/L]	[ng/L]	[ng/L]	[ng/L]	[ng/L]	[ng/L]	[ng/L]	[ng/L]	[ng/L]	[ng/L]	[ng/L]	[ng/L]	[ng/L]			
High springs																		
LT-1	0.44	1.16	0.69	0.91	1.26	1.49	1.71	1.70	2.09	2.26	2.25	2.63	2.80	3.25	3.48	2.05	0.17	1.21
LT-2	0.72	1.58	1.19	1.53	1.68	1.86	1.66	1.40	1.53	1.28	1.56	1.77	1.88	2.34	2.51	1.50	0.45	1.27
Low springs																		
CG-6	1.28	0.92	1.18	1.20	1.10	1.13	1.08	0.86	0.88	0.93	0.81	0.86	0.77	0.75	0.85	0.63	1.15	1.07
Streams																		
CG-4	0.88	0.60	0.95	1.00	0.91	0.95	0.89	0.81	0.77	0.88	0.80	0.78	0.81	0.81		0.44	0.79	1.31
Retention in soluble phase																		
High springs																		
LT-1	61%	66%	77%	65%	70%	82%	67%	84%	65%	70%	78%	72%	84%	71%	85%	68%	79%	>90%
LT-2	55%	54%	70%	62%	71%	79%	69%	>90%	66%	67%	>90%	74%	>90%	74%	>90%	85%	84%	>90%
Low springs																		
CG-6	64%	59%	76%	71%	76%	78%	75%	87%	79%	77%	84%	77%	>90%	82%	85%	>90%	87%	>90%
Streams																		
CG-4	52%	38%	61%	57%	69%	79%	60%	81%	69%	66%	83%	71%	>90%	65%		88%	82%	>90%

4 DISCUSSION

4.1 REE behavior in water

Measured rare earth element concentrations for springs and streams are presented in Table 2. To compare results with other REE studies of various lithological settings, I plotted REE patterns normalized to the commonly used Post Archaean Australian Shale (PAAS) as well as a local basalt from White et al. (1993) (Figures 2a-c and 2d-f respectively). $[La/Yb]_{PAAS}$ and $[Eu/Eu^*]_{PAAS}$ show similar ranges when comparing to other studies of small stream catchments draining basaltic lithologies, with depletion of LREE and a lower total REE compared to felsic rocks (Saunders, 1984; Steinmann and Stille, 2008; Johannesson et al., 2017). No major MREE enrichment was observed, with relatively flat patterns between Gd and Yb. Because apatite is often enriched in MREEs, the lack of such an enrichment demonstrates that apatite weathering is not a major component of the chemical weathering fluxes of REEs in this system (Leybourne and Johannesson, 2008; Xu and Han, 2009). This observation is consistent with the low P_2O_5 concentrations in the bedrock basalts (White et al., 1993). Studies of REE in natural waters often consider possible anthropogenic input, mainly Gd (Bau and Dulksi, 1996; Song et al., 2017; Johannesson et al., 2017; Smith and Liu, 2018). Specifically, Gd is a key component in Magnetic Resonance Imaging (MRI) facilities in hospitals (Bau and Dulski, 1996). However, no positive Gd anomaly was observed (Figure 2a-c), demonstrating the lack of human-induced REE input or fractionation in this location.

To investigate processes specific to chemical weathering of the local catchment, normalization to basalt REE patterns allow for investigation of fractionation processes from bedrock to dissolved load. Most low-elevation spring and stream samples exhibit roughly flat REE patterns, suggesting relatively stable REE release from bedrock sources. High-elevation springs, however, show a strong peak at Ce and general depletion in LREEs, indicating that some other factor other than release from bedrock must determine REE concentrations in the dissolved load. The same high-elevation spring samples also display

a strong LREE depletion, in addition to other stream samples which show weak LREE depletion. These two identified deviations from bedrock REE patterns will be discussed further in Sections 4.2 and 4.3.

4.2 Ce anomaly (Ce/Ce*)

Considering that Ce is preferentially removed from the "dissolved" load via adsorption to particles enhanced by its 4+ valence state, it is rare to observe a positive Ce anomaly ($[Ce/Ce^*]_b > 1$) in naturally oxidized freshwater systems. For this to occur, Ce (IV) must be preferentially incorporated in the "dissolved" load relative to other trivalent LREEs. Anoxic (reducing) conditions could favor Ce existing primarily in its trivalent state and behaving similarly to its neighbors La and Pr. However, this would only result in $[Ce/Ce^*]_b = 1$ without a mechanism to specifically isolate Ce. It is also possible that cerianite (CeO_2) formed from oxidative scavenging of Ce and later re-dissolved under acidic conditions, but this explanation also would not satisfy the observation of a positive Ce anomaly. Because the positive Ce anomaly persists in the soluble phase, colloidal/soluble partitioning cannot sufficiently explain this observation.

The samples with $[Ce/Ce^*]_b > 1$ were all pristine, dilute, low-pH springs with high Mn concentrations (Figure 3). It is proposed that low molecular weight Mn colloids are responsible for scavenging Ce and concentrating it into the "dissolved" and soluble phase. Mn has been observed to exist in completely dissolved (ionic) form for several days after entering oxidizing conditions before precipitating out of solution (Hem, 1963). It can be assumed then, that Mn oxides should be allowed to exist in the colloidal and even soluble phase of the water samples. Even without microbes present to facilitate oxidative scavenging, Ce has a much higher affinity for MnO_2 than its neighbors La and Pr, with partition coefficients 1-2 orders of magnitude lower for the trivalent REEs (Koeppenkastrop and DeCarlo, 1992; DeCarlo and Wen, 1998; Ohta and Kowabe, 2001). This is especially true for acidic solutions, where anionic complexing agents are less abundant (Johannesson et al., 1995). Fe-oxyhydroxides, on the other hand, does not preferentially scavenge Ce compared to other LREEs (DeCarlo and Wen, 1998). As pH increases and Mn oxides will either bind together to >0.45μm particulate sizes or, more likely, co-

precipitate with Fe-oxyhydroxides as they become more stable at higher pH. The high-elevation springs are shown to retain most Mn in the soluble phase due to their low pH, with lower elevation samples bearing most Mn in the colloidal or suspended phase (Figure 4). Mn is removed from soluble to the colloidal and suspended phase downstream with increasing pH, causing a return to negative values ($[Ce/Ce^*]_b$ 0.58-1.02) as Ce switches to the more typical behavior in freshwater systems - removal from the "dissolved" load due to oxidative scavenging.

Mn oxides have also demonstrated a slightly higher efficiency at scavenging HREEs from solution at sufficiently low pH (Ohta and Kowabe, 2001). Assuming Mn oxide colloids are responsible for the observed positive Ce anomaly, it is reasonable to expect that the high concentration of Mn oxides will enrich the "dissolved" and even the soluble load in HREEs. This also explains the relatively low $[La/Yb]_b$ values for high-elevation Mn-rich springs. Consequently, calculated Ce anomaly values are more pronounced because LREEs are actively depleted relative to HREEs by the same mechanism that attracts Ce, showing a higher value for $[Ce/Ce^*]_b$ both because of elevated Ce concentrations and diminished LREE concentrations.

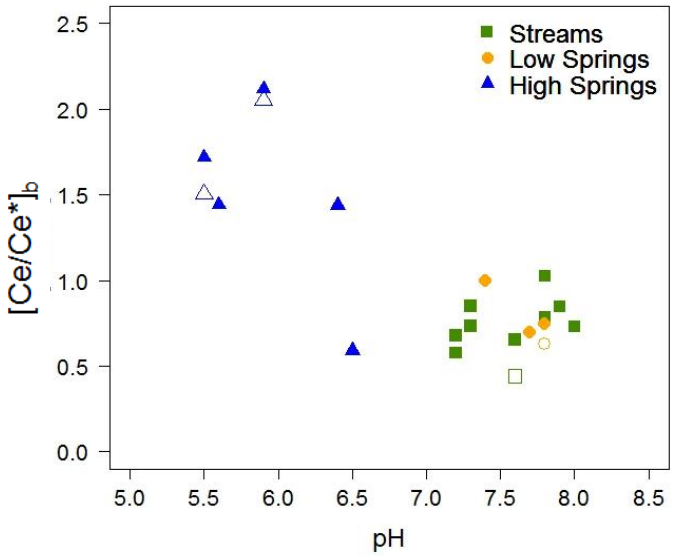

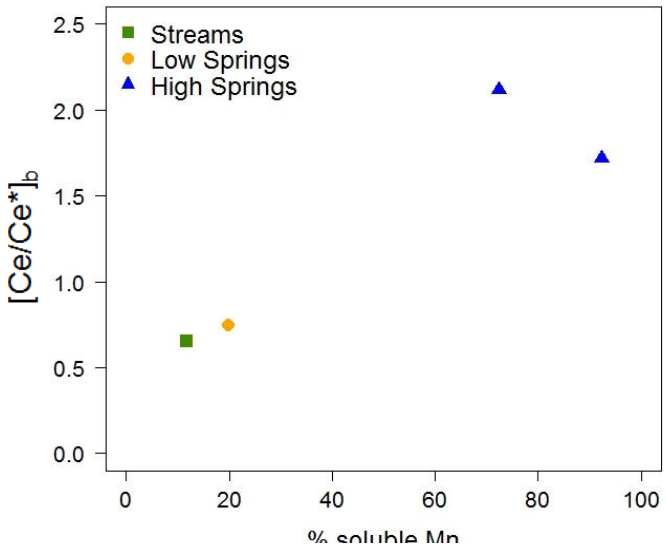

Figure 3: shows Ce anomaly ($[Ce/Ce^*]_b$) values for all samples plotted over pH. Values for the 0.02µm filtered samples are shown as empty points.
Figure 4: shows Ce anomaly over % soluble Mn from Table 3a

4.3 LREE to HREE Ratios (La/Yb)

The pH dependence of REE fractionation has been thoroughly explored in major world rivers and laboratory settings (Sholkovitz 1992, 1995; Bau et al. 1999). Generally, pH determines relative REE adsorption: the preferential scavenging of REEs changes from LREEs to HREEs as pH increases. A positive trend for spring samples is observed in $[La/Yb]_b$ as a function of pH, while stream samples show wide variability for a narrow range of pH (Figure 5).

Fe-oxyhydroxide colloids have been repeatedly reported with sizes smaller than .45μm or even .02μm (Andersson et al., 2006; Flynn, 1984), an observation which is consistent with the high concentrations of Fe observed in the soluble load (Figure 6). It seems likely that the increase in pH in the groundwater samples is enough to encourage the formation colloidal Fe-oxyhydroxides (SI > 1 for most low-elevation samples), without aggregating to be greater than 0.45μm particle size. I observed that LREEs are preferentially incorporated into the colloidal and truly dissolved phase because of their high affinity for newly-formed Fe-oxyhydroxides (Figures 5 and 6) with increasing pH and SI of Fe-oxyhydroxides. Pokrovksy and Schott (2002) suggest that these colloidal Fe-oxyhydroxide scavengers of trace elements often form by reduction of Fe (II) to Fe (III) at the boundary between anoxic groundwater and oxidizing surface conditions.

Stream samples show a positive correlation between $[La/Yb]_b$ and P concentration (Figure 7). As the watershed evolves and the stream outlet is reached, $[La/Yb]_b$ values return to ~0.5 as P is reduced as well. One possible explanation is vegetation-induced removal of LREEs from the dissolved load, showing a correlation with dissolved P because of its status as a bio-limiting nutrient (Cleveland et al., 2002). Several studies have shown that LREEs are preferentially taken into plant structures (Stille and Steinmann, 2006; Liang et al., 2008). This explanation does not fit with the data presented here (decreasing $[La/Yb]_b$ with decreasing P downstream) because 1). the climatic gradient causes vegetation to decrease with elevation towards the coast, which would cause an increase in LREE enrichment downstream; 2). no correlation was found between DOC and either $[La/Yb]_b$ or P. A more likely explanation is that Fe-oxyhydroxide colloids have aggregated and removed LREEs from the dissolved

load, consistent with the decrease in % retention of Fe in the sequentially filtered stream sample (Table 3). Alternatively, the simultaneous depletion of LREEs and dissolved P could be attributed to the progressive precipitation of the secondary mineral rhabdophane or other REE-bearing phosphates, which have been proven to preferentially incorporate LREEs during formation (Banfield and Eggleton, 1987; Johannesson et al., 1995; Leybourne and Johannesson 2008). This increase in LREE removal due to secondary phosphate mineral precipitation accompanies a sharp decrease in chemical weathering rates along the climatological gradient of the island. This might reduce the input of P into the dissolved load which might push the system out of equilibrium and encourage phosphate precipitation.

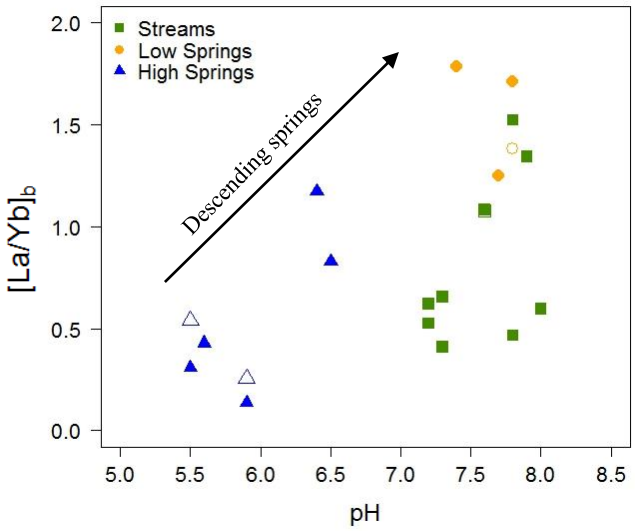

Figure 5 (top left): LREE enrichment $[La/Yb]_b$ plotted over pH with 0.02µm filtered values as empty points
Figure 6 (bottom left): LREE enrichment over % retention of Fe in the soluble phase
Figure 7 (bottom right): LREE enrichment plotted over measured P concentration

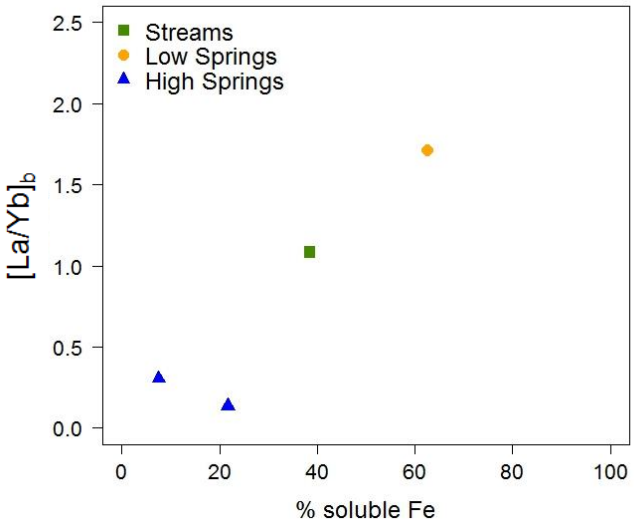

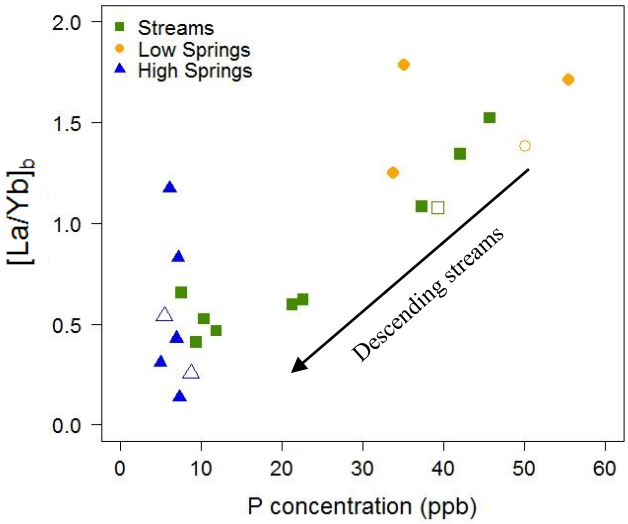

5 CONCLUSIONS

This study presents the REE concentrations of groundwater spring and stream samples on San Cristóbal Island across a sharp hydrologic gradient. This gradient is primarily manifested as a steep increase in pH, resulting in a shift between Mn-dominated to Fe-dominated mineralogy in colloidal solutions. These variations are accompanied by pronounced REE fractionation, consistent with laboratory studies performed over wide ranges of pH and particulate mineralogy.

1. Following sequential filtration through 0.45μm and 0.02μm size filters, it is observed that LREEs have a higher affinity for the colloidal (0.02μm-0.45μm) vs. the soluble (<0.02μm) phase.
2. The positive Ce anomaly observed in acidic high-elevation groundwater springs is attributed to soluble/colloidal Mn scavenging and retaining Ce in the "dissolved" load. Furthermore, Mn oxides fractionate HREEs relative to LREEs and cause a more pronounced Ce anomaly as a result of depletion of La and Pr.
3. Progressive LREE enrichment is observed as pH increases in groundwater springs, marking the shift into Fe-dominated colloids as Fe-oxyhydroxides become thermodynamically stable. The trend is especially clear in groundwater spring samples because there is insufficient oxidative conditions to cause Fe-oxyhydroxides to bind together and exceed .45μm in size. Colloidal Fe-oxyhydroxides enrich LREEs in the "dissolved" phase.
4. The gradual LREE depletion with stream evolution (i.e. as distance from catchment outlet decreases) is mostly likely due to one of two mechanisms, either a). Fe-oxyhydroxides aggregate and exceed .45μm, removing LREEs from the "dissolved" phase into the suspended phase, or b). secondary phosphate minerals like rhabdophane precipitate out of solution and incorporate LREE preferentially into the suspended phase.

ACKNOWLEDGEMENTS

I would like to thank my advisor, Dr. Xiaoming Liu, who has supervised this project and taught me how to independently approach the entire scientific process. I could not have done this work without Dr. Diego Riveros-Iregui, who guided me through the process of fieldwork and worked with logistics of sample transportation. I would like to acknowledge the field assistance of Emily Browning and Sarah McQueen, laboratory help from Cheng Cao, Wenshuai Li, and Heather Hanna, and expert field advice from Madelyn Percy. Finally, I would like to recognize support from the Pignatiello Fund (UNC Department of Geological Sciences) and the McGee Family Travel Fund (UNC Office for Undergraduate Research).

BIBLIOGRAPHY

Adelinet, M., Fortin, J., D'Ozouville, N., & Violette, S. (2008). The relationship between hydrodynamic properties and weathering of soils derived from volcanic rocks, Galapagos Islands (Ecuador). *Environmental Geology*. *56*(1), 45-58.

Allègre, C., Dupré, B., Négrel, P., & Gaillardet, J. (1996). Sr-Nd-Pb isotope systematics in Amazon and Congo River systems: constraints about erosion processes. *Chemical Geology, 131*(1-4), 93-112.

Andersson, K., Dahlqvist, R., Turner, D., Stolpe, B., Larsson, T., Ingri, J., & Andersson, P. (2006). Colloidal rare earth elements in a boreal river: Changing sources and distributions during the spring flood. *Geochimica et Cosmochimica Acta, 70*(13), 3261-3274.

Arsouze, T., Dutay, J.-C., Lacan, F., & Jeandel, C. (2009). Reconstructing the Nd oceanic cycle using a coupled dynamical – biogeochemical model. *Biogeosciences, 6*(12), 2829-2846.

Banfield, J., & Eggleton, R. (1989). Apatite replacement and rare earth mobilization, fractionation, and fixation during weathering. *Clays and Clay Minerals, 37*(2), 113-127.

Bau, M. (1999). Scavenging of dissolved yttrium and rare earths by precipitating iron oxyhydroxide: experimental evidence for Ce oxidation, Y-Ho fractionation, and lanthanide tetrad effect. *Geochimica et Cosmochimica Acta, 63*(1), 67-77.

Bau, M., & Dulski, P. (1996). Anthropogenic origin of positive gadolinium anomalies in river waters. *Earth and Planetary Science Letters, 143*(1-4), 245-255.

Bertram, C., & Elderfield, H. (1993). The geochemical balance of the rare earth elements and neodymium isotopes in the oceans. *Geochimica et Cosmochimica Acta, 57*(9), 1957-1986.

Cantrell, K., & Byrne, R. (1987). Rare earth element complexation by carbonate and oxalate ions. *Geochimica et Cosmochimica Acta, 51*(3), 597-605.

Cidu, R., & Biddau, R. (2007). Transport of trace elements under different seasonal conditions: Effects on the quality of river water in a Mediterranean area. *Applied Geochemistry, 22*(12), 2777-2794.

De Carlo, E., Wen, X.-Y., & Irving, M. (1997). The Influence of Redox Reactions on the Uptake of Dissolved Ce by Suspended Fe and Mn Oxide Particles. *Aquatic Geochemistry, 3*(4), 357-389.

Dia, A., Gruau, G., Olivié-Lauquet, G., Riou, C., Molénat, J., & Curmi, P. (2000). The distribution of rare earth elements in groundwaters: assessing the role of source-rock composition, redox changes and colloidal particles. *Geochimica et Cosmochimica Acta, 64*(24), 4131-4151.

Dupré, B., Gaillardet, J., Rousseau, D., & Allègre, C. (1996). Major and trace elements of river-borne material: The Congo Basin. *Geochimica et Cosmochimica Acta, 60*(8), 1301-1321.

Gaillardet, J., Dupre, B., Allegre, C., & Négrel, P. (1997). Chemical and physical denudation in the Amazon River Basin. *Chemical Geology, 142*(3-4), 141-173.

Geist, D., McBirney, A., & Duncan, R. (1986). Geology and petrogenesis of lavas from San Cristobal Island, Galapagos Archipelago (Pacific). *97*(5), 555-566.

Goldstein, S., & Jacobsen, S. (1987). The Nd and Sr isotopic systematics of river-water dissolved material: Implications for the sources of Nd and Sr in seawater. *Chemical Geology: Isotope Geoscience section, 66*(3-4), 245-272.

Goldstein, S., & Jacobsen, S. (1988). Rare earth elements in river waters. *Earth and Planetary Science Letters, 89*(1), 35-47.

Hannigan, R., & Sholkovitz, E. (2001). The development of middle rare earth element enrichments in freshwaters: Weathering of phosphate minerals. *Chemical Geology*.

Hem, J. (1963). Chemical equilibria and rates of manganese oxidation. *Water Supply Paper*.

Hey, R., & Vogt, P. (1977). SPREADING CENTER JUMPS AND SUB-AXIAL ASTHENOSPHERE FLOW NEAR THE GALAPAGOS HOTSPOT *. *Tectonophysics, 37,* 41-52.

Huttel, Charles, Winckell, Alain, Pourrut, Pierre, . . . Loaiza. (1989). Inventario cartografico de los recursos naturales, geomorfologia, vegetacion, hidricos, ecologicos y biofisicos de las islas Galapagos Ecuador.

Johannesson, K. H., Lyons, W. B., Stetzenbach, K. J., & Byrne, R. H. (1995). The solubility control of rare earth elements in natural terrestrial waters and the significance of PO 4 3− and CO 3 2− in limiting dissolved rare earth concentrations: A review of recent information. *Aquatic Geochemistry, 1*(2), 157-173.

Johannesson, K., Lyons, W., Stetzenbach, K., & Byrne, R. (1995). The solubility control of rare earth elements in natural terrestrial waters and the significance of PO 4 3? and CO 3 2? in limiting dissolved rare earth concentrations: A review of recent information. *Aquatic Geochemistry, 1*(2), 157-173.

Johannesson, K., Palmore, C., Fackrell, J., Prouty, N., Swarzenski, P., Chevis, D., . . . Burdige, D. (2017). Rare earth element behavior during groundwater–seawater mixing along the Kona Coast of Hawaii. *Geochimica et Cosmochimica Acta, 198,* 229-258.

Johannesson, K., Zhou, X., Guo, C., Stetzenbach, K., & Hodge, V. (2000). Origin of rare earth element signatures in groundwaters of circumneutral pH from southern Nevada and eastern California, USA. *Chemical Geology, 164*(3-4), 239-257.

Kato, Y., Nakao, K., & Isozaki, Y. (2002). Geochemistry of Late Permian to Early Triassic pelagic cherts from southwest Japan: implications for an oceanic redox change. *Chemical Geology, 182*(1), 15-34.

Koeppenkastrop, D., & De Carlo, E. (1992). Sorption of rare-earth elements from seawater onto synthetic mineral particles: An experimental approach 1. *Chemical Geology, 95,* 251-263.

Leybourne, M., & Johannesson, K. (2008). Rare earth elements (REE) and yttrium in stream waters, stream sediments, and Fe–Mn oxyhydroxides: Fractionation, speciation, and controls over REE + Y patterns in the surface environment. *Geochimica et Cosmochimica Acta, 72*(24), 5962-5983.

Liu, H., Pourret, O., Guo, H., & Bonhoure, J. (2017). Rare earth elements sorption to iron oxyhydroxide: Model development and application to groundwater. *Applied Geochemistry, 87,* 158-166.

Liu, Y.-G., Miah, M., & Schmitt, R. (1988). Cerium: A chemical tracer for paleo-oceanic redox conditions. *Geochimica et Cosmochimica Acta, 52*(6), 1361-1371.

Murray, R., Buchholtz ten Brink, M., Jones, D., Gerlach, D., & Russ III, G. (1990). Rare earth elements as indicators of different marine depositional environments in chert and shale. *Geology, 18*(3), 268.

Ohta, A., & Kawabe, I. (2001). REE(III) adsorption onto Mn dioxide (δ-MnO2) and Fe oxyhydroxide: Ce(III) oxidation by δ-MnO2. *Geochimica et Cosmochimica Acta, 65*(5), 695-703.

Percy, M. S., Schmitt, S. R., Riveros-Iregui, D. A., & Mirus, B. B. (2016). The Galápagos archipelago: a natural laboratory to examine sharp hydroclimatic, geologic and anthropogenic gradients. *Wiley Interdisciplinary Reviews: Water*, *3*(4), 587-600.

Pokrovsky, O., & Schott, J. (2002). Iron colloids/organic matter associated transport of major and trace elements in small boreal rivers and their estuaries (NW Russia). *Chemical Geology, 190*(1-4), 141-179.

Pryet, A., D'Ozouville, N., Violette, S., Deffontaines, B., & Auken, E. (2012). Hydrogeological settings of a volcanic island (San Cristobal, Galapagos) from joint interpretation of airborne electromagnetics and geomorphological observations. *Hydrology and Earth System Sciences*.

Saunders, A. (1984). The Rare Earth Element Characteristics of Igneous Rocks from the Ocean Basins. *Developments in Geochemistry, 2*, 205-236.

Sholkovitz, E. (1995). The aquatic chemistry of rare earth elements in rivers and estuaries. *Aquatic Geochemistry, 1*(1), 1-34.

Smith, C., & Liu, X.-M. (2018). Spatial and temporal distribution of rare earth elements in the Neuse River, North Carolina. *Chemical Geology*.

Song, H., Shin, W.-J., Ryu, J.-S., Shin, H., Chung, H., & Lee, K.-S. (2017). Anthropogenic rare earth elements and their spatial distributions in the Han River, South Korea. *Chemosphere, 172*, 155-165.

Steinmann, M., & Stille, P. (2008). Controls on transport and fractionation of the rare earth elements in stream water of a mixed basaltic-granitic catchment basin (Massif Central, France). *Chemical Geology*.

Stille, P., Steinmann, M., Pierret, M.-C., Gauthier-Lafaye, F., Chabaux, F., Viville, D., . . . Aubert, D. (2006). The impact of vegetation on REE fractionation in stream waters of a small forested catchment (the Strengbach case). *Geochimica et Cosmochimica Acta, 70*(13), 3217-3230.

Tachikawa, K., Athias, V., & Jeandel, C. (2003). Neodymium budget in the modern ocean and paleo-oceanographic implications. *Journal of Geophysical Research: Oceans, 108*(C8).

Taylor, S., & McLennan, S. (1985). *The Continental Crust: Its Composition and Evolution. An Examination of the Geochemical Record Preserved in Sedimentary Rocks.* Blackwell Scientific Publications, Oxford.

Violette, S., D'Ozouville, N., Pryet, A., Deffontaines, B., Fortin, J., & Adelinet, M. (2014). Hydrogeology of the Galápagos Archipelago: An Integrated and Comparative Approach Between Islands. In S. Violette, N. D'Ozouville, A. Pryet, B. Deffontaines, J. Fortin, & M. Adelinet, *The Galapagos: A Natural Laboratory for the Earth Sciences.*

Warrier, R., Castro, M., & Hall, C. (2012). Recharge and source-water insights from the Galapagos Islands using noble gases and stable isotopes. *Water Resources Research*.

White, W., McBirney, A., & Duncan, R. (1993). Petrology and geochemistry of the Galápagos Islands: Portrait of a pathological mantle plume. *Journal of Geophysical Research: Solid Earth, 98*(B11), 19533-19563.

Wood, S. (1990). The aqueous geochemistry of the rare-earth elements and yttrium: 1. Review of available low-temperature data for inorganic complexes and the inorganic REE speciation of natural waters. *Chemical Geology, 82*, 159-186.

Xu, Z., & Han, G. (2009). Rare earth elements (REE) of dissolved and suspended loads in the Xijiang River, South China. *Applied Geochemistry, 24*(9), 1803-1816.